

Generating building-level heat demand time series by combining occupancy simulations and thermal modeling

Simon Malacek^{a,b}, José Portela^c, Yannick Werner^a, Sonja Wogrin^{a,b}

^a Institute of Electricity Economics and Energy Innovation at Graz University of Technology, Inffeldgasse 18, Graz, 8010, Austria

^b Research Center ENERGETIC, Rechbauerstraße 12, Graz, 8010, Austria

^c Instituto de Investigación Tecnológica (IIT), Universidad Pontificia Comillas, Calle Alberto Aguilera 23, Madrid, 28015, Spain

ARTICLE INFO

Keywords:

Public data
Thermal building model
Building occupancy
Synthetic heat demand time series
Single building resolution

ABSTRACT

Despite various efforts, decarbonizing the heating sector remains a significant challenge. To tackle it by smart planning, the availability of highly resolved heating demand data is key. Several existing models provide heating demand only for specific applications. Typically, they either offer time series for a larger area or annual demand data on a building level, but not both simultaneously. Additionally, the diversity in heating demand across different buildings is often not considered. To address these limitations, this paper presents a novel method for generating temporally resolved heat demand time series at the building level using publicly available data. The approach integrates a thermal building model with stochastic occupancy simulations that account for variability in user behavior. As a result, the tool serves as a cost-effective resource for cross-sectoral energy system planning and policy development, particularly with a focus on the heating sector. The obtained data can be used to assess the impact of renovation and retrofitting strategies, or to analyze district heating expansion. To illustrate the potential applications of this approach, we conducted a case study in Puertollano (Spain), where we prepared a dataset of heating demand with hourly resolution for each of 9,298 residential buildings. This data was then used to compare two different pathways for the thermal renovation of these buildings. By relying on publicly available data, this method can be adapted and applied to various European regions, offering broad usability in energy system optimization and analysis of decarbonization strategies.

1. Introduction

Within the European Union (EU), the residential sector accounts for approximately 28% of the final energy consumption as of 2021 [1]. Of this, more than 78% is used for space heating and hot water treatment [2]. Despite efforts to decarbonize the heat supply, 77% of this energy demand still comes from non-renewable sources [3], which contributes to about one-third of energy-related greenhouse gas emissions. The EU Energy Performance of Buildings Directive EU/2024/1275 [4] aims to reduce emissions from this sector by at least 60% by 2030 compared to 2015 levels, making it a crucial part of the EU's overall climate targets.

To address this challenge, the main pathways for reducing residential energy consumption are clear:

- improving building insulation to reduce heating demand [5],
- expanding district heating systems,
- and replacing oil- and gas-fired boilers with heat pumps alongside with increasing the share of renewables in the power system [6].

The required technologies and devices are available at a mature level and low costs [7].

While the general strategy described above seems conceptually simple, its real-world implementation presents significant challenges. Boosting the thermal renovation of buildings and retrofitting heating systems requires well-targeted policies [8]. Moreover, ongoing electrification of heating systems will increase the overall power demand, potentially leading to higher peak loads [9]. This could necessitate grid reinforcements to ensure stability and additional expansion of renewable power production [10].

Successfully transforming the building sector at minimal economic cost requires a smart, integrated planning and design approach [11]. This approach must consider the coupling of the heating and power sectors, as well as retrofitting measures that impact the distribution of loads. One critical requirement of this planning is access to accurate, high-resolution data on heating demand in both space and time domain [12].

* Corresponding author at: Institute of Electricity Economics and Energy Innovation at Graz University of Technology, Inffeldgasse 18, Graz, 8010, Austria.

E-mail address: simon.malacek@tugraz.at (S. Malacek).

URL: <https://iee.tugraz.at> (S. Malacek).

Abbreviations

GIS	Geographic information system
HDD	Heating degree days
INSPIRE	Infrastructure for spatial information in the European community
LIDAR	Light detection and ranging
MCMC	Markov–chain monte carlo
NUTS	Nomenclature of territorial units for statistics
OSM	Open street maps
RC model	Resistor-capacitor model
TUS	Time use survey

Nomenclature

i	Index for buildings
t	Index for the time steps
$A(t)$	Active occupancy at time step t
AHD	Annual heating demand
G	Generalized thermal conductance
k	Generalized thermal storage capacity
$Q_{\text{demand}}(t)$	Required heating demand for time step t
$Q_{\text{heating}}(t)$	Actual applied heating power for time step t
$Q_{\text{heating,max}}$	Maximum heating power
$Q_{\text{losses}}(t)$	Thermal losses at time step t
Q_i	Yearly heating demand for building i
$Q_{\text{spec},i}$	Specific heating demand for building i
S_i	Residential area of building i
$T_{\text{in}}(t)$	Indoor temperature for time step t
$T_{\text{out}}(t)$	Outside temperature for time step t
$T_{\text{set,daytime}}$	Setpoint temperature at daytime
$T_{\text{set,nighttime}}$	Setpoint temperature at nighttime

On the one hand, high spatial resolution of heating demand data, e.g. at the building level, allows for the identification of the most effective renovation measures and enables the design of well-targeted policies like subsidy programs. This high spatial resolution is also essential when assessing the economic viability of district heating networks [13]. On the other hand, high temporal resolution, e.g. hourly resolved heat demand time series, enables the analysis of the impact of heating system electrification on the power grid [14]. By considering the additional electrical loads (e.g. from heat pumps) and analyzing the impact of thermal load shifting on the power system, these data can inform decisions for sector-coupled generation and expansion planning in integrated power and heat systems. For example, focusing on the integration of district heating systems [15] or energy hubs [16]. Together that shows that cost-efficient system planning and optimization strongly rely on granular data. This is often available (for research purposes) for the power sector as smart meter measurements at the building or household level, distribution network data, and national energy statistics, all with hourly or even quarter-hourly resolution. However, this level of detail is not yet available for heat load curves at any scale. Existing methodologies (discussed in detail in Section 1.1) and data sources for heating demand provide either geolocated annual heating demand, synthetic load profiles for individual buildings, or aggregated load curves for specific regions based on gas or district heating consumption.

Only a few methodologies [17–19] generate both hourly load profiles at a high spatial resolution. However, none of these approaches fully accounts for the stochastic nature of load profiles caused by diverse and asynchronous user behavior across different buildings. Furthermore, only a few are based solely on easily accessible open-source data. We discuss the most relevant methods in the following section.

1.1. Review of existing methods in literature

A wide range of approaches for modeling thermal demand can be found in the literature, each with different objectives. We summarize the key methods, focusing on spatially-oriented approaches in Section 1.1.1 and temporally-oriented methods in Section 1.1.2. Finally, Section 1.1.3 explores approaches integrating spatial and temporal perspectives.

1.1.1. Methods for spatial heating demand data

The literature typically distinguishes top-down and bottom-up approaches for generating heating demand data [20,21]. Top-down approaches, such as the one used by Gils et al. [22], disaggregate the total heating demand of a defined region by weighting it with predefined parameters, most commonly population density. The total heating demand is either measured directly (e.g., through gas or electricity consumption) or derived from economic energy statistics. These models are relatively simple to implement when the necessary data is available. However, their spatial resolution is limited because statistical data cannot be traced down to the level of individual buildings, making them suitable for large-scale analyses but less effective for district-level planning tasks.

With the increasing availability of open data sources, more bottom-up approaches have emerged. These models start at the smallest unit, usually buildings or even individual households. Geographic Information Systems (GIS) data, such as OpenStreetMap (OSM) [23], are often utilized to geolocate buildings. Some studies also incorporate 3D building data (e.g., Schwanbeck et al. [24] for Germany) or LIDAR data (e.g. [25] in Vitoria-Gasteiz, Spain) to perform more sophisticated analyses of building volumes. On the building level, the yearly heating demand is typically calculated based on residential area and a typical specific heating energy demand for that building type. Residential areas can be estimated from GIS data [26–28] or from cadastral and census information [29].

To obtain the specific heating energy demand for buildings, they are often categorized into different archetypes (i.e. types of representative buildings for a region). The TABULA Web Tool [30] is commonly used as the data source for this. The tool provides specific heating energy demand values (in kWh yr^{-1}) based on factors such as the country (which dictates national building standards), climate zone, building type (e.g., single-family house, terraced house, apartment block), and construction year. Some studies, like that of Dall'O' et al. [31], validate the building data through energy audits of sample buildings.

Beyond this standard approach, some models consider additional input parameters. For example, the Building Thermal Energy Assessment Model by Prades-Gil et al. [32] includes solar irradiation, which has been found to significantly impact specific energy demand, second only to climate variables [33]. Martín-Consuegra [29] also incorporates the facade area, allowing for higher spatial resolution even within building blocks.

Several studies compare the results of bottom-up and top-down methods. Meha et al. [34] performed such a comparison for a test region in Kosovo. Calderón et al. [35] calculated the end-use energy demand at the building level for the UK by combining top-down and bottom-up methods, focusing on national energy planning. Parnpuri et al. [36] employed a methodology that uses energy performance certificates from Switzerland's database along with building age to calculate yearly demand. They validated the results by comparing the summed demands with statistical data on energy consumption at the canton level. All of these studies demonstrated a strong alignment between the top-down and bottom-up methodologies.

In addition to presenting different modeling approaches and individual case studies, several projects provide heating demand data at the European level. Notable examples include the Pan-European Thermal Atlas (PETA) [37], developed as part of the *Heat Roadmap Europe* project [38], and the *sEnergies* project. The *Hotmaps Toolbox* [39]

offers similar outputs and validates derived heating demands within reference cities. National projects, such as the *MapaDeCalor* [40] for Spain, also provide useful heating demand data. While these maps allow for easy access to heating demands and related information, such as waste heat potentials at a regional level or integrated calculation tools, their spatial resolution is too coarse for district-level planning, where street or building-level resolution is required.

The bottom-up approaches discussed above are particularly useful when actual measured heating demand data is unavailable. They are often applied to assess the potential for retrofitting [28] or to expand district heating systems. For instance, Nielsen and Möller [26] used a heat map (energy demand per building) of Denmark to assess the economic feasibility of district heating networks in new neighborhoods. Additionally, these approaches can be used to analyze energy poverty, as demonstrated by Terés-Zubiaga et al. [41] at the building level. By focusing on retrofitting efforts, such studies can not only help achieve ecological goals but also generate social benefits by addressing energy poverty, reducing carbon emissions, and improving living conditions.

1.1.2. Methods for temporal heat load profiles

Various approaches exist for generating load profiles, which can be broadly categorized into data-driven black-box models and engineering white-box models based on physical equations and detailed individual building data. Further categorization of these approaches is discussed in the Supplementary Material of Staffell et al. [33]. Simple, previously used, standard load profiles are no longer applicable for smart energy planning at the district level, as discussed in [17]. An extensive review of the various methods, available software packages, and their different fields of application is provided by Jebaraj and Iniyar [42] and more recently by Allegrini et al. [43]. Peacock's review from 2021 [44] analyses four common modeling approaches, including the Heating Degree Days (HDD) method, and compares them with actual measured data. The review shows that all methods yield good results, but they only provide daily temporal resolution.

Data-driven models require minimal information about the actual physical parameters of buildings. However, they do rely on measured heating demands, typically obtained from existing district heating networks or gas consumption data [45]. These models often aim to predict future consumption in existing district heating networks or perform correlation analyses between heating demand and external variables such as temperature. For example, Dang et al. analyzed heat load patterns in existing district heating systems, emphasizing the importance of considering not just thermal building parameters and outside temperature [46], but also, in a subsequent work, user behavior for accurate predictions [47]. Similarly, Maljkovic and Basic [48] explored the influence of various parameters on heating demand using machine learning, measured data, and surveys. Fumo and Biswas [49] provide a review of regression analysis for predicting residential energy consumption, highlighting the simplicity of regression models compared to physical models for demand prediction. However, when no data is available, one must rely on engineering or physical models instead.

Engineering models, such as EnergyPlus [50], are well-established tools for detailed simulations based on energy balance equations and physical parameters. These models can provide sub-hourly resolved load profiles for individual buildings. However, due to the need for highly detailed parameters, these models are not suitable for whole cities or large areas. Additionally, they typically do not account for varying occupancy patterns across different buildings. As a result, simply adding up the simulated profiles of multiple buildings (as in [18]) can lead to unrealistic aggregated load peaks.

To address the issue of artificial load peaks, stochastic models have been introduced. Palacios-Garcia et al. [51] present a stochastic modeling and simulation approach for (electric) heating and cooling demand. Fischer et al. [52] also use a stochastic bottom-up model to estimate load profiles for space heating and hot water demands. Stochasticity in these models refers to incorporating randomness alongside physical

modeling, which better reflects the individual asynchronous behavior of building occupants.

Stochastic properties can be implemented using the Markov-Chain Monte Carlo (MCMC) method, a standard approach for random sampling. One of the first to incorporate this into load profile synthesis was Richardson et al. [53], who emphasized the importance of user behavior in accurately modeling heating and electricity demand. They proposed a methodology based on Time Use Surveys (TUS) [54] to generate active occupancy profiles for integration into demand models. A similar approach was employed by Ding et al. [55] to generate temporal occupancy profiles even on a room level. Furthermore, a more sophisticated analysis of occupancy behavior, considering demographic and household characteristics, was discussed by Fu et al. [56], suggesting a more detailed approach to modeling occupancy patterns.

At the database level, the *When2Heat* project (original publication [57], current version of the dataset [58]) provides demand data and other parameters, such as the coefficient of performance for heat pumps, for several European countries. This comprehensive database offers quick and easy access to valid load profiles. However, these data are aggregated at a $0.75^\circ \times 0.75^\circ$ grid level, which does not provide sub-district level spatial resolution.

1.1.3. Combined approaches

Several studies [17,45,59] have discussed the advantages of obtaining heating demand data with both high spatial and temporal resolution, presenting various approaches to achieve this.

Berger and Worlitschek [59] provide a case study with heating demand data at a spatial resolution of one square kilometer for all of Switzerland, but with a temporal resolution limited to one day, based on the HDD method. They propose a top-down methodology to generate aggregated load curves, combining population density distribution maps, norm temperature profiles, HDDs, and total (measured or statistical) residential heating demand. In contrast, Koene and Eslami-Mossallam [45] use an electrical equivalent resistor-capacitor (RC) model to generate hourly heating load profiles, comparing them with gas consumption data. However, the spatial resolution is limited to the district level, and thermal properties are estimated from the gas demand signature (top-down), rather than being derived from individual building data. This approach is therefore unsuitable for districts with no known gas or district heating demand, such as those without district heating systems or those utilizing diverse decentralized technologies like wood, oil ovens, and heat pumps.

Some studies offer spatially and temporally resolved data for specific regions, but not at the building level: Malla [19], in his master's thesis, recognizes the need for high spatial and temporal resolution in heat demand profiles and presents a methodology to calculate load profiles for a $100\text{ m} \times 100\text{ m}$ grid across Germany. Clegg and Mancarella [60] developed a method with a half-hourly resolution for 404 areas of Great Britain. While they validate their time series against measured gas consumption data, the spatial resolution remains at the district level. Lombardi et al. [12] present a thermodynamic modeling approach for Italian regions, incorporating many physical details for heat transfer to build an accurate model. However, the spatial resolution is limited to the NUTS-2 [61] level (corresponds to regions/provinces). Their model (with available code) also enables running different refurbishment scenarios defined by the user.

Recently, Staffell et al. proposed a global model for hourly heating and cooling demands [33], which provides temporally resolved load profiles for locations worldwide. However, not on a building-level. These profiles are publicly available on [62], though they need to be scaled according to the actual yearly heating demand of the region of interest.

An interesting approach by Büttner et al. [17] applies a top-down methodology, disaggregating census data down to the building level. Each building is assigned a pre-generated load profile from a set of 1259 different profiles based on its properties. However, this top-down

approach distributes heating demand evenly across all buildings within a given cell, regardless of the actual building type. As a result, the method is not capable of capturing variability between buildings within a district.

Finally, Heidenthaler et al. [18] uses energy performance certificates and a simulation tool to generate load profiles at the building level. However, this model does not account for the stochastic nature of user behavior, leading to unrealistic peaks in heating demand.

1.2. Original contribution

The literature review highlights the variety of existing methods and approaches, each with a specific scope of application and inherent limitations. For instance, traditional building energy models can produce highly precise and, when properly calibrated, accurate heat demand time series for individual buildings or small building clusters. However, they require detailed input data – such as building geometry, orientation, wall structure, construction materials, and insulation characteristics – which may not be readily available for large-scale applications. In contrast, regression-based models can provide reasonable estimates at aggregated levels (e.g., district or city scale), but they typically lack the spatial granularity required to resolve heat demand at the individual building level.

To the best of our knowledge, none of the existing approaches can generate stochastic heat demand time series at the building level using only publicly available data for a large number of buildings. While individual features have been implemented into existing models, none of them combine all these elements into a unified framework. However, such integration is essential to enable the straightforward generation of heat demand data in data-scarce contexts, supporting a wide range of applications in energy system modeling — particularly those focusing on sector coupling with high spatial resolution, such as the planning of local heat networks for waste heat utilization. To address this methodological gap, we present a novel approach that integrates the following distinct features into a single workflow:

1. **Publicly Available Data Utilization** — Tailoring the workflow to work exclusively with publicly available data ensures broad applicability and superior scalability, enabling analysis of thousands of buildings and overcoming data shortages.
2. **Simplified Physics-Based Thermal Model** — Using a physics-based model allows for the generation of reasonable demand profiles at the individual building level, making the method independent of standard load profiles, disaggregation techniques, or previously measured profiles.
3. **Stochastic Occupancy Simulation** — Incorporating user behavior and utilizing stochastic simulation ensures realistic demand profiles that account for household asynchronicity and demand fluctuations, while maintaining scalability from a single neighborhood to entire regions.

This novel approach enables the flexible generation of high-resolution heat demand data with minimal input requirements — supporting the decarbonization of heat supply across diverse regions. Although showcased through a specific case study, the method is widely applicable and highly scalable, offering a powerful tool for data-driven energy system planning.

1.3. Organization of the remainder of this paper

Section 2 provides a detailed explanation of the data sources and methods used, followed by validation results in Section 2.3. The subsequent case study (Section 3) applies the methodology to a city in Spain, highlighting the importance of the resulting data and its potential applications. The discussion on these applications, along with the limitations and possible areas for further improvements, can be found in Section 4.

2. Methodology

In this section, we present a methodology to generate hourly heat demand profiles on the single building level based on publicly accessible data and considering the stochasticity of user behavior. The process is designed to work with a minimum input of publicly available data, ensuring broad applicability. By that, it provides valuable data for various energy analyses across different fields of research, particularly where this data is currently lacking or unavailable.

After discussing different data sources in 2.1, each step of the model is explained in detail in Sections 2.2.1–2.2.6. Subsequently, Section 2.3 illustrates the validity of the method using several comparative and analytic approaches.

2.1. Data sources

Table 1 provides an overview of the required data for the proposed model and lists publicly available data sources. The references cited in the **Source** column of Table 1 provide data within the EU. However, the accuracy and completeness of the data can vary for different countries and locations. Any other source providing similar data can be used for the following steps.

2.2. Data processing

The following paragraphs describe the data processing, which can be subdivided into the following six steps:

- Step 1: Acquire geo-data, including the buildings with shape information and GPS location.
- Step 2: Request data from a cadaster/census data source for every building.
- Step 3: Categorize every building according to a building typology.
- Step 4: Estimate the thermal properties of every building.
- Step 5: Generate load profiles by considering user behavior by MCMC method and the thermal building model.
- Step 6: Aggregate data for subsequent applications (if necessary).

Fig. 1 illustrates the corresponding workflow and data sources.

2.2.1. Step 1: Geo-data conditioning

To begin, the region of interest for the analysis is identified. OpenStreetMap (OSM) [23] serves as a robust source of geospatial data, providing structured geoinformation. This typically includes a (geo)object for each building, containing at least its centroid GPS location and shape, and often additional attributes such as postal address, building height, or usage type. Moreover, OSM frequently covers other infrastructure, such as streets and electricity grids, which can be valuable for further analysis. Data for the selected region can be downloaded directly or obtained using tools like Overpass Turbo [64], which facilitates additional filtering and preprocessing. Subsequently, the structured geodata must be transformed into a tabular format, where each row corresponds to a building and includes its associated parameters.

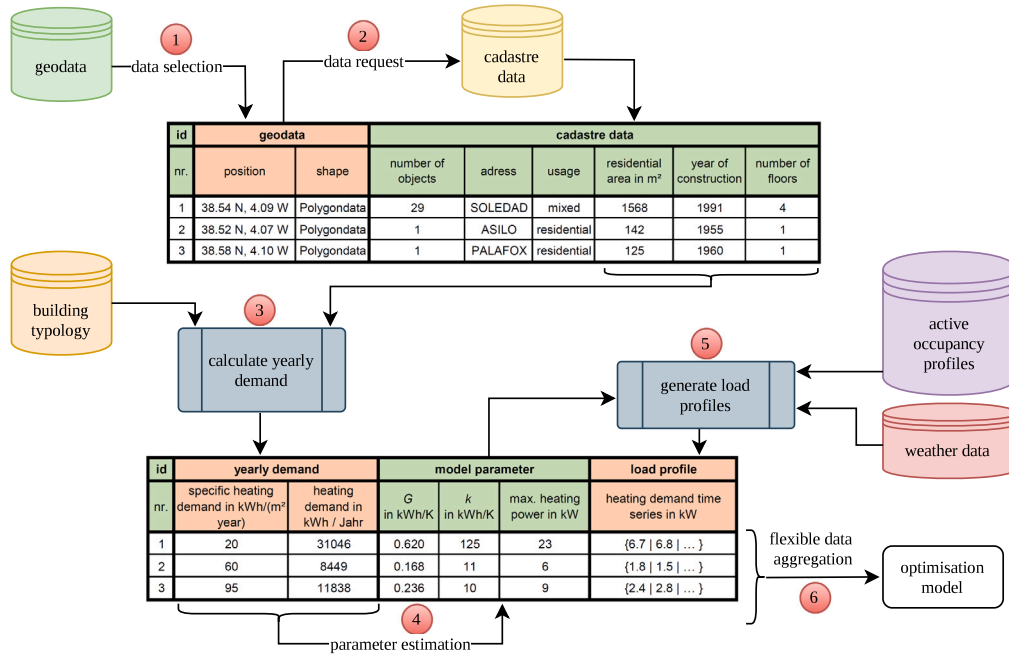
2.2.2. Step 2: Cadaster data request

The EU directive 2007/2/EG, passed in 2007 [63], aims to ensure the provision of comprehensive geospatial information across the EU. To achieve this, INSPIRE (Infrastructure for Spatial Information in the European Community) was established, enabling access to cadastral data in all member states. While the specific implementation varies by country and region, options such as bulk downloads or individual data requests based on address, cadastral reference, or GPS location are generally available. Ideally, these datasets provide information at the building level, including the number of units, usage type, year of construction, and (residential) area S_f . If such data is unavailable, it can be approximated using alternative parameters: The area can

Table 1

Data sources for the subsequent generation of spatial-temporal resolved heat demand profiles.

Type	Description	Source
Geodata	Location and shape of buildings	Open Street Maps [23]
Cadaster data	Number of units and number of floors, year of construction, (residential) area, address, type of usage	INSPIRE [63]
Building typology	Specific heating demand	TABULA WebTool [30]
Active occupancy profiles	Activity statistics and time profiles	TUS [54]
Weather data	Hourly resolved outdoor temperature	Renewable.ninja [62]

**Fig. 1.** Schematic illustration of required data sources and the data processing workflow. The enumerated steps correspond to the steps in Section 2.2.1.

be estimated from the building's shape and height, as demonstrated in Ref. [25]. For buildings with missing construction year data, a default yearly heating demand, representing a weighted average, is assigned in the subsequent steps. These fallback assumptions enhance the method's robustness against missing data entries. However, each additional estimation introduces a potential source of uncertainty. To quantify this error margin, the Supplemental Material [65] compares results from cadastral data with the simplified estimation based solely on OSM, showing that the difference in yearly heating demand amounts to 14%. To apply our method, this information is retrieved from the cadastral records and appended to each building entry in the dataset.

2.2.3. Step 3: Determination of yearly heating demands

A straightforward approach identifies three key parameters that primarily influence a building's heating energy demand: (i) **Location**: The country and climate zone determine the climatic conditions, including the outside temperature and heating degree days. Additionally, the building's energy performance standards are often tied to its geographic location. (ii) **Year of Construction**: This reflects the thermal performance legislation, typical building standards, and construction methods in place at the time the building was erected. (iii) **Building Type**: The classification (e.g., single-family house, terraced house, apartment block) influences the volume-to-envelope ratio. A higher ratio, indicative of a more compact design, generally results in better thermal performance. The TABULA Web Tool [30] supports this analysis by providing a detailed typology that categorizes buildings based on these parameters and offers specific heating energy demand estimates.

Using this data, each building in the dataset can be classified, yielding a specific heating demand, $Q_{\text{spec},i}$, for each building. The total

residential heating demand, Q_i , for a building is then calculated by scaling the specific heating demand with its residential area, S_i , using: $Q_i = S_i Q_{\text{spec},i}$.

2.2.4. Step 4: Estimation of thermal properties

In real-world scenarios involving large numbers of buildings, detailed data on construction materials, wall thicknesses, and window types is often unavailable. To address this, we implemented a simplified thermal model, as illustrated in Fig. 2.

In this model:

- Thermal losses**, including transmission through walls, floors, roofs, and ventilation, are represented by a single parameter for each building i : the thermal conductance G_i (in kW K^{-1}). In the absence of more detailed data, this parameter is estimated by dividing the total annual heating demand for the respective building AHD_i by the cumulative indoor-outdoor temperature difference over all hours of the year:

$$G_i = \frac{\text{AHD}_i}{\sum_{t|T_{\text{set}}(t) > T_{\text{out}}(t)} (T_{\text{set}}(t) - T_{\text{out}}(t))} \quad \forall i \quad (1)$$

- Thermal storage capacity**, k (in kWh K^{-1}), is assumed based on average values for typical construction materials and wall thicknesses [66], scaled according to building size. While more detailed distinctions could be made using building type and construction year, the marginal improvement in accuracy may not justify the significantly increased effort to track specific materials for every building.

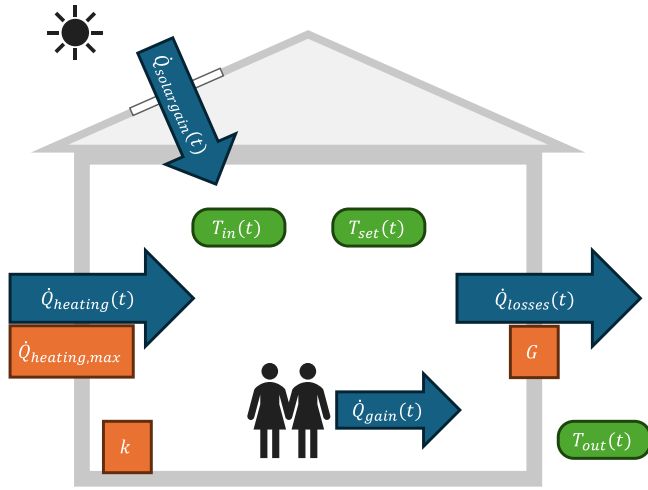


Fig. 2. Thermal model for generating heating demand load profiles. $T_{in}(t)$ = hourly actual indoor temperature in °C, $T_{out}(t)$ = hourly outdoor temperature in °C, $T_{set}(t)$ = hourly set temperature based on occupancy and daytime in °C, k = thermal storage capacity in kWhK^{-1} , G = thermal conductance in kWK^{-1} , $\dot{Q}_{heating,max}$ = maximum heating power in kW, $\dot{Q}_{losses}(t)$ = heat losses in kW, $\dot{Q}_{gain}(t)$ = heat gain by internal sources in kW, $\dot{Q}_{solargain}(t)$ = heat gain by solar irradiation in kW, $\dot{Q}_{heating}(t)$ = actual heating power in kW.

- **Maximum heating power**, $\dot{Q}_{heating,max}$ (in kW), is determined using a standard method for heating system dimensioning [67], independent of the heating supply type.

The simplifications outlined for estimating thermal properties are intended to ensure broad applicability across diverse scenarios. However, if more detailed data is available for a specific analysis, it can be incorporated to replace the simplified assumptions and enhance the accuracy of the results.

2.2.5. Step 5: Synthetic load profile generation

The hourly heating demand is influenced not only by the thermal properties of the building and the outside temperature but also significantly by the indoor setpoint temperature. For this analysis, we assume the setpoint temperatures of individual dwellings follow a normal distribution around $T_{set,daytime} = 21^\circ\text{C}$ for daytime and $T_{set,nighttime} = 16^\circ\text{C}$ for nighttime with a standard deviation of $\pm 2^\circ\text{C}$ for both. To account for the temporal variation in setpoint temperatures, we introduce the concept of active occupancy. When residents are at home and active, the temperature is set to $T_{set,daytime}$; otherwise, it is reduced when residents are either away (e.g., at work or school) or inactive (e.g., sleeping).

This behavior is represented by a Boolean variable $A(t)$:

- $A(t) = \text{true}$ indicates the residents are active and at home.
- $A(t) = \text{false}$ means the residents are either away or inactive.

The general distribution of active occupancy can be derived from Time Use Surveys [54], which are regularly conducted across European countries. These surveys capture daily routines through empirical questionnaires administered to a statistically representative sample population. However, applying a single, uniform time profile for all buildings in the thermal model would not accurately reflect real-world variability, as people do not wake up or follow their daily routines at the same time. To address this, the MCMC method [53] is used to generate individual active occupancy profiles $A_i(t)$ for each dwelling i . In an MCMC chain, the next state $A(t+1)$ depends only on the current state $A(t)$ and is determined by a transition matrix specific to the time step, with a randomness factor introduced for transitions. Different transition matrices are used for weekdays and weekends to

reflect workday-dependent behavior. The randomness in the generated profiles captures individual variability in daily routines. Nevertheless, the average of a sufficiently large number of profiles converges to the distribution derived from TUS data. A detailed implementation of the MCMC method, including sample data and validation, can be found in the Supplementary Materials [65].

Fig. 3 illustrates this process, showing individual generated profiles (Fig. 3(a)) and the average of many profiles (Fig. 3(b)), converging for large sample numbers to the overall desired distribution. It should be noted that due to the stochastic nature of MCMC, the individual profiles will differ with each simulation run. However, this does not impact the aggregated results. In cases where reproducibility is desired (e.g., to obtain consistent numbers for testing), each building can be assigned a seed number, to produce a reproducible series of random numbers.

Once the active occupancy profiles are determined, the temperatures and thermal flows can be calculated using a quasi-static, time-discrete model with hourly time steps Δt . The thermal losses $\dot{Q}_{losses}(t)$ for each hour are computed using Eq. (2), which is based on the difference between the current indoor temperature and the outdoor temperature, multiplied by the generalized thermal conductance G :

$$\dot{Q}_{losses}(t) = G \cdot (T_{in}(t) - T_{out}(t)) \quad (2)$$

Having determined the active occupancy profiles, the setpoint temperature for each time interval T_{set} is directly derived from the active occupancy and the statistically distributed parameters $T_{set,daytime}$ and $T_{set,nighttime}$, as shown in Eq. (3), which are fixed for each model run.

$$T_{set} = \begin{cases} T_{set,daytime}, & \text{if } A(t) = \text{true} \\ T_{set,nighttime}, & \text{if } A(t) = \text{false} \end{cases} \quad (3)$$

To calculate the actual current indoor temperature $T_{in}(t)$, the total heat provided by heating $\dot{Q}_{heating}(t-1)$, plus internal gains $\dot{Q}_{gain}(t-1)$ and solar gains $\dot{Q}_{solargain}(t-1)$, minus the thermal losses $\dot{Q}_{losses}(t-1)$ from the previous time step, is divided by the thermal capacity k of the building and added to the previous indoor temperature $T_{in}(t-1)$ (see Eq. (4)). Internal gains arise from the use of electrical appliances, cooking, or the body heat of occupants. Depending on the available information and the required level of detail, a constant contribution can be assumed [45], the profile can be linked to active occupancy [52], or it can be derived from empirical measurements [68]. In our approach, the magnitude of internal gains per building is scaled by the number of dwellings. Solar gains account for the thermal energy received by the building from solar radiation. This contribution can be roughly estimated using hourly irradiation and window area, as discussed in [20] and Section 2.5. Initial values of $\dot{Q}_{heating}(t=0) = 0$ and $T_{in}(t=0) = T_{set}$ are chosen.

$$T_{in}(t) = T_{in}(t-1) + \Delta t \frac{\dot{Q}_{heating}(t-1) + \dot{Q}_{gain}(t-1) + \dot{Q}_{solargain}(t-1) - \dot{Q}_{losses}(t-1)}{k} \quad (4)$$

Knowing the indoor temperature, the required amount of energy $\Delta Q(t)$ to heat the building to T_{set} can be calculated as the thermal capacity k times the temperature difference (see Eq. (5)).

$$\Delta Q(t) = k \cdot (T_{set}(t) - T_{in}(t)) \quad (5)$$

By adding the thermal losses, the total heating demand for that particular time step $\dot{Q}_{demand}(t)$ is calculated as:

$$\dot{Q}_{demand}(t) = \dot{Q}_{losses}(t) + \frac{\Delta Q(t)}{\Delta t} \quad (6)$$

Finally, the actual heating demand is determined by a case differentiation in Eq. (7). If the calculation results in a negative value for a particular hour, it is set to zero. Otherwise, a negative heating demand would imply a decrease in indoor temperature, which does not reflect real-world conditions. Additionally, a maximum heating power

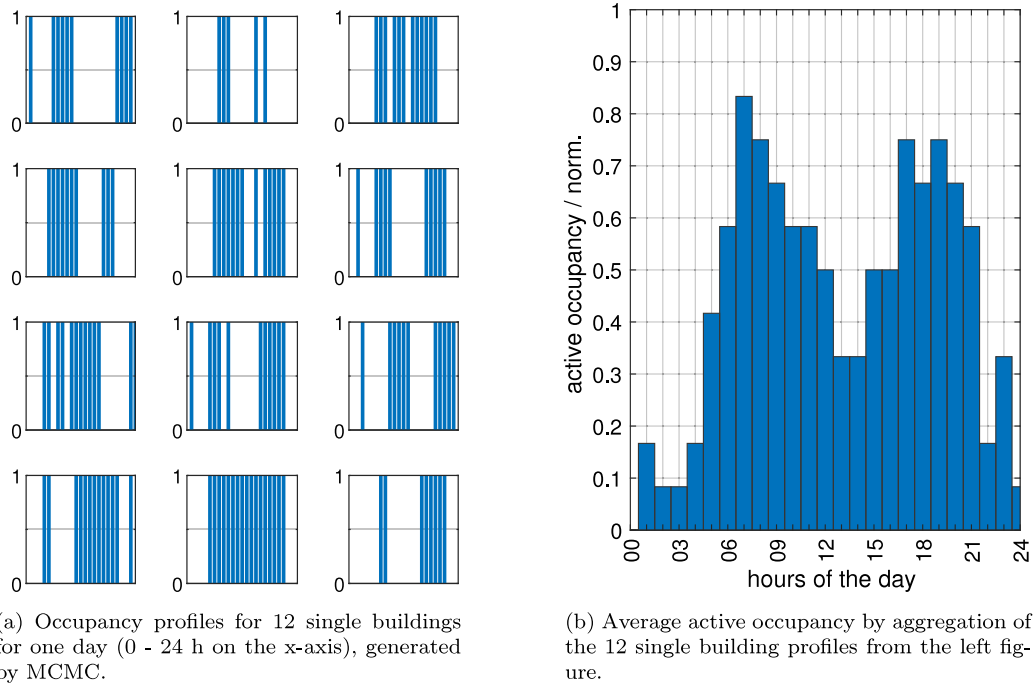


Fig. 3. Illustration of the convergence of single discrete active occupancy profiles (a), towards an average active occupancy profile (b).

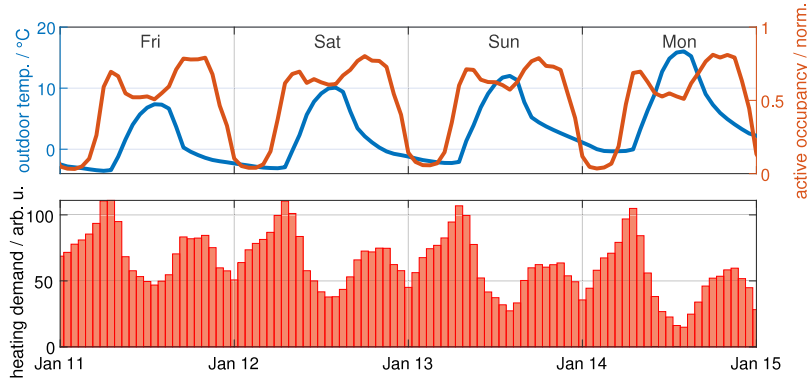


Fig. 4. Relation between heating demand and the outside temperature and active occupancy. Peaks in the heating demand correlate with low outside temperature and high active occupancy, leading to the characteristic morning and evening peaks.

$\dot{Q}_{\text{heating,max}}$ is introduced to limit the added heat per unit time, better representing a real system setup.

$$\dot{Q}_{\text{heating}}(t) = \begin{cases} 0 & \text{if } \dot{Q}_{\text{demand}} < 0 \\ \dot{Q}_{\text{demand}}(t) & \text{if } 0 < \dot{Q}_{\text{demand}} < \dot{Q}_{\text{heating,max}} \\ \dot{Q}_{\text{heating,max}} & \text{if } \dot{Q}_{\text{demand}} > \dot{Q}_{\text{heating,max}} \end{cases} \quad (7)$$

Through iterative calculations, a time series (e.g., for one year with 8760 h) can be generated, yielding an individual heating demand \dot{Q}_{heating} for every building. Fig. 4 illustrates an example of such a heating demand profile and its dependency on the outside temperature and active occupancy.

2.2.6. Step 6: Flexible data aggregation

The heating demand profiles obtained at the building level can now be directly applied for further data analysis, or incorporated into simulations or optimization models. Using one of the various methods for network generation, such as minimum spanning tree for previously clustered buildings [69] or at the individual building level [25], a district heating network topology can be proposed. Based on this topology, the load profiles can be easily aggregated by summing all the profiles

from a particular branch, thereby drastically reducing computational effort.

Additionally, these thermal load profiles can be translated into electricity demands by assuming the use of electric boilers or heat pumps for heating in the building. The high spatial resolution of the data allows for the assignment of the additional power demand to specific distribution grid nodes. This enables an analysis of the impact of expansion decisions for the heating system (such as whether to connect to the district heating network or use a heat pump or electric boiler) on the overall system. Both the electric grid and the district heating system, along with their respective thermal demands, are accounted for. This approach facilitates the identification of the cross-sectoral optimal solution for each building.

While the annual heating demand calculated by our method is deterministic for each individual building, the corresponding time series exhibit stochastic variations due to the MCMC-based occupancy modeling. By aggregating time series, individual patterns are smoothed out, leading to a convergence towards a common distribution. Since only the active occupancy profiles themselves have a stochastic component, it can be assumed that the stochastically influenced part of the heat profiles will converge in the same manner (i.e., by aggregating

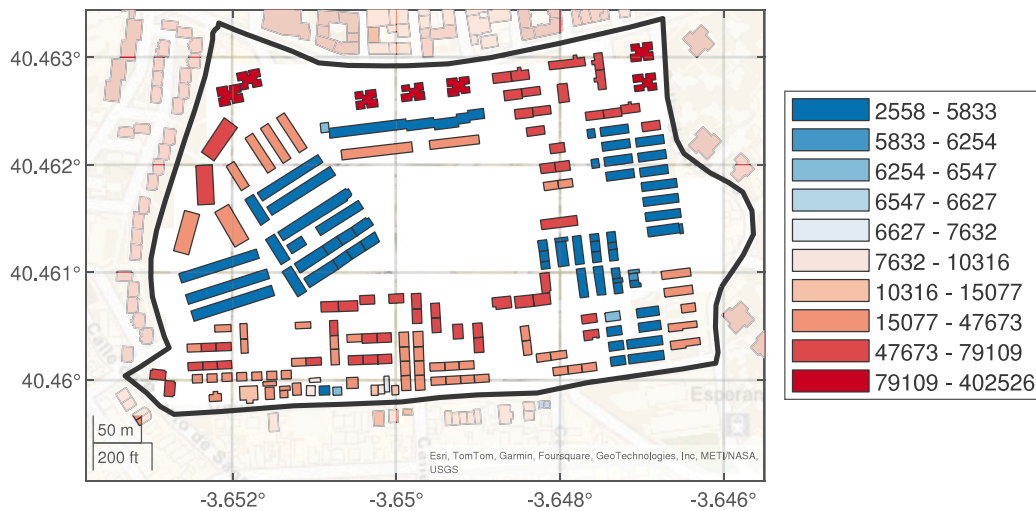


Fig. 5. Yearly heating demand on building level in kWhyr^{-1} . For better comparison, the color scale was adapted to Ref. [29]. (For interpretation of the references to color in this figure legend, the reader is referred to the web version of this article.)

approximately 10 dwelling profiles, as shown in the Supplementary Material [65]). Any remaining differences in the aggregated heat demand time series are primarily caused by variations in the respective building stock.

2.3. Validation

We validate the results obtained by our method in three key ways: First, by comparing the results with those of another study in 2.3.1, we demonstrate the reasonableness of the heating demand at the building level. Second, in 2.3.2, we show the correlation between heating demand and temperature, confirming the correct distribution of the daily heating demand throughout the year. Finally, in Section 2.3.3, we compare the hourly intra-day profiles generated by our method to demonstrate their strong agreement with the intra-day distributions reported in the literature.

2.3.1. Replication analysis

To illustrate that our methodology retrieves the correct yearly heating demand at the building level, we applied it (up to step 3, see Section 2.2.3) to a quarter in Madrid, which was analyzed in a study by Martín-Consuegra (Ref. [29]). Fig. 5 shows our results. For better comparison, the color codes were selected according to Figure 6 in the original publication Ref. [29]. Although fewer details at the sub-building level are resolved, the heating demand at the whole building level aligns well, demonstrating good accordance between the methodologies at the single-building resolution.

2.3.2. Correlation analysis

The daily heating demand shows a strong correlation with the daily average outside temperature, as described in the literature, such as in Ref. [33]. Fig. 6 demonstrates that this expected correlation can also be found in the data obtained through our methodology. Additionally, accounting for occupancy results in higher heating demand on weekends compared to weekdays with similar outside temperatures. Conversely, the variability in heating demand for days with similar outside temperatures is attributed to the thermal inertia of the buildings, which is reproduced by our model. Together, these findings suggest reasonable results at a daily-based temporal scale.

2.3.3. Comparison of daily profiles

A critical aspect of heating demand time series for planning applications is providing reasonable intra-day resolution. However, methods like the HDD approach do not offer this, and data from physical models can result in unrealistic load peaks when the profiles are simply aggregated. To validate the hourly heating demand data from our method, Fig. 7 compares the average daily profile with a measured profile from Ref. [45]. The typical double-peak structure in the heating demand, as also reported in Ref. [60], is clearly visible, with the highest heating demand occurring in the morning and evening when most people are at home and temperatures are still low or have dropped again. In addition to this generic structure, the shape of the profile depends on the location of the city and the corresponding outside temperature profile. While the upper subplot in Fig. 7 shows data from the Netherlands (with generally lower daytime temperatures), the lower subplot displays the demand profile of a city in Spain. Despite this, the comparison demonstrates that our method provides a reasonable intra-day resolution.

2.4. Comparison with other methodologies

As discussed in the Introduction 1.1.2, a variety of different approaches for time series generation exists. In Fig. 8, we compare our results with data from a few commonly used methods, specifically:

- HDD: standard heating degree days method, expanded for hourly resolution.
- Renewables.ninja: data from Ref. [33], calculated by an advanced heating degree days method, that includes additional parameters.
- Physical model: data from a building simulation software. Simulations were performed for three building types, and added with weights, representing the share of the building type.

The left tile shows demand during a winter day, where the shortcomings of simply aggregating data from physical models are evident. Due to the lack of a stochastic factor, all demand occurs simultaneously, producing unrealistic peaks. In the right tile, a late summer day is depicted: With warm temperatures during the day, all methods that consider thermal inertia result in no or very low heating demand. In contrast, the HDD method, which solely considers the outside temperature and neglects historical information, provides a non-zero value for the heating demand.

Both Renewables.ninja and our method address the systematic limitations mentioned above. However, it appears that Renewables.ninja

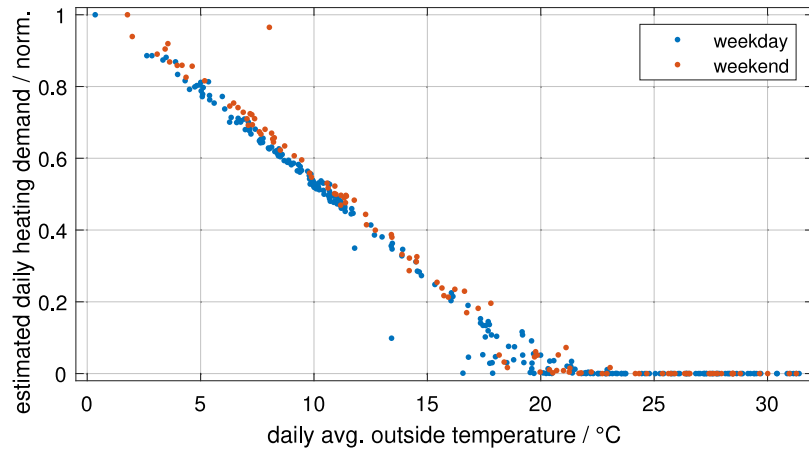


Fig. 6. Correlation analysis between estimated daily heating demand and daily average outside temperature.

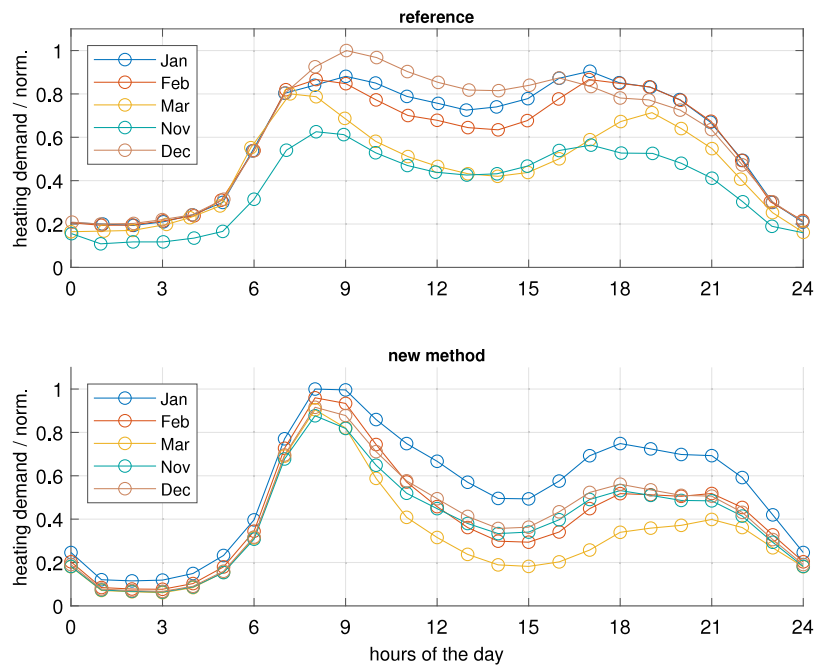


Fig. 7. Comparison of average daily heating demand profiles. The upper tile (reference), shows actual measured heating demand data from Ref. [45], in comparison, the lower tile shows results obtained by our methodology. In addition to location-based deviations, the generic shape aligns, demonstrating the reasonableness of our data.

underestimates the impact of user behavior, as the heating demand during nighttime is only slightly lower than during peak hours. In contrast, our model combines the strengths of both approaches by accurately accounting for thermal physics and the stochastic effects of diversity among different buildings. As a result, the data generated by our model seems to represent a convolution of the physical model and the outcomes from Renewables.ninja.

2.5. Methodical and data uncertainty

Although our method produces accurate heating demand profiles at an aggregated level, it is important to emphasize that each independent load profile at the building level represents a random sample, derived from overall statistical data and assumed building properties. As such, it does not necessarily exactly match the heating demand of a specifically given building. Since the primary goal of this methodology is to generate data for large-scale analyses rather than to design individual heating systems for specific buildings, this limitation does not significantly affect the overall results.

As with any modeling approach, the quality of input data is critical to the accuracy of the output. For heating demand at the building level, uncertainties arise from incomplete or outdated data in GIS/OSM or cadaster systems, as well as from ambiguities in the assignment of building archetypes, as discussed by Dochev et al. [70]. However, Dochev et al. also note that such discrepancies tend to average out when considering aggregated data. For a specific application in a case study, we strongly encourage researchers applying this method to carefully examine the input data and conduct plausibility checks and sample validations.

Potential systematic errors may also arise from neglecting additional factors, such as solar irradiation, urban heat islands, wind chill, internal heat gains from the human body, lighting, cooking, other electrical appliances, or varying individual setpoint temperatures and ventilation habits. Nonetheless, Staffell et al. [33] demonstrate that, in their model, most of these factors have only a minor effect, with solar gain being the most significant. In comparison, the impact of these factors is generally smaller than the uncertainty introduced by the input data.

For projects that require precise solar gain calculations, more detailed building models are necessary. Accurately assessing shading

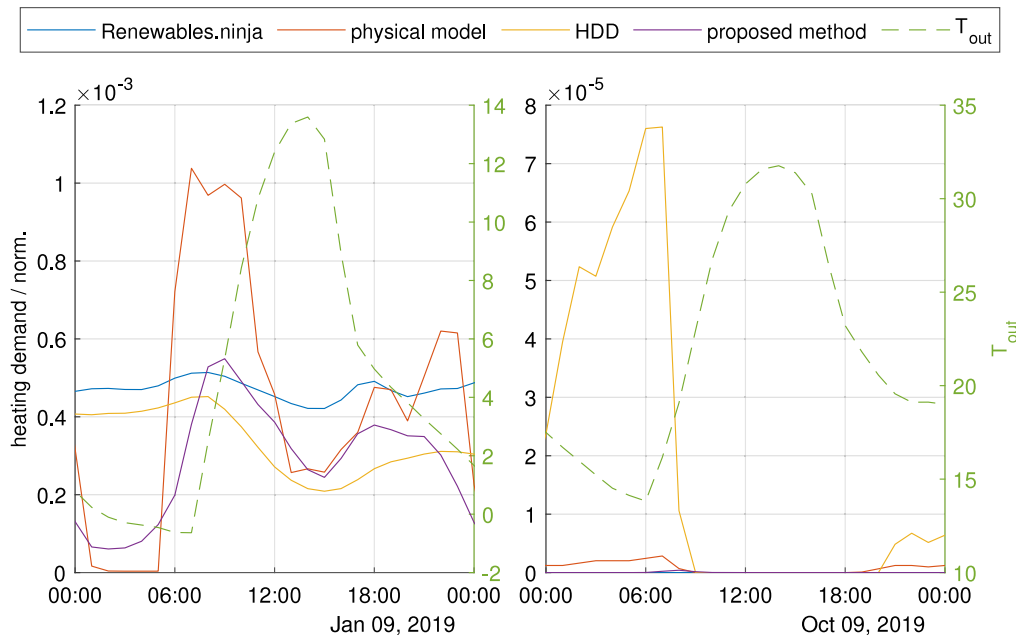


Fig. 8. Comparison of different methodologies for generating heating demand profiles for a winter (left) and summer (right) day. Profiles are normalized to the yearly sum (same annual heating demand).

effects and the amount of effective solar radiation reaching buildings requires consideration of building shapes, orientation, morphology, roof shapes and window openings [20]. Such analyses typically rely on highly detailed building data, including 3D models. These models are also crucial for evaluating the impact of urban heat islands [71], which, as reported by [72], can change the heating demand of individual buildings by up to 20%. However, comprehensive 3D building data is not yet widely accessible to the public. Therefore, we have deliberately chosen a simplified model, acknowledging a certain degree of uncertainty while ensuring broad and universal applicability of our approach. Beyond that, it is worth noting that variations between different climate years may result in larger deviations than the factors discussed above.

3. Case study: Analyzing the heating demand of Puertollano/Spain

Following a brief motivation for selecting this particular case and an introduction to the context in Section 3.1, we describe the application of our methodology to Puertollano in Section 3.2. The results obtained are presented and discussed in Section 3.3, with an emphasis on the value of the datasets for smart planning applications.

It is important to note that the applicability of the proposed method is not limited to this case study. This analysis illustrates the general structure of the obtained data and represents just one of many possible applications.

3.1. Motivation and aim of the case study

In 2022, one of the largest electrolyzers in Europe was commissioned in Puertollano, Spain. This electrolyzer, with a nominal electric input power of 20MW, is powered by a 100MW photovoltaic (PV) park located nearby [73]. With the planned addition of 200MW of electrolyzer capacity, the region is set to become a key European hydrogen hub. As part of this project, it was proposed to utilize the waste heat from the electrolyzer, at a temperature of 56 °C, for district heating to provide affordable heat to up to 3000 households [74].

Given the lower temperature level and the potential intermittency related to solar irradiation and electrolyzer operational schedule, a more advanced planning approach is required compared to traditional heat engineering methods for network design. Sector-coupled optimization models are a leading tool for assessing the technical and economic

feasibility of such projects and determining the optimal system configuration. However, detailed heating demand time series at a granular spatial level are essential for comprehensive analysis.

In this case study, we demonstrate that our methodology is capable of generating such plausible synthetic load profiles at the building level, using publicly available data. Beyond the application for this particular analysis, these profiles serve as a reliable foundation for further analyses, such as, optimizing strategies for decarbonizing heating systems, or determining future additional electricity load profiles, particularly in scenarios involving the partial or full electrification of heating demand.

3.2. Data analysis

For the Puertollano case study, the initial dataset for the region was sourced from OSM [23], which provides details on various infrastructures, including 11 725 buildings, of these, 9298 are residential buildings. Each building object contains information about the centroid location, shape (defined by GPS coordinates), and height recorded.

Subsequent to this, additional building-specific data was obtained from the Spanish cadaster [75] using the provided API [76]. This dataset includes information on building usage type, construction year, area designation, number of units, and postal address. For buildings containing multiple units (e.g. apartment buildings), data for each individual subobject (household) was requested and aggregated at the building level. A sample of this data at the building level is presented in Fig. 9. Due to the lack of detailed 3D building information and building-specific window areas, solar gains are not considered in this case study, such that $Q_{\text{solar gain}} = 0$ in Eq. (4). This simplification avoids introducing additional uncertainty from estimated or assumed solar exposure parameters, which would require complex geometric modeling and accurate material properties that are typically not available from open data sources.

To estimate the specific annual heating demand, the information on the year of construction, number of units, and number of floors was combined with typological data from the TABULA Webtool [30]. For this analysis, a continental climate was selected, and heating demand data for both original and retrofitted buildings was extracted separately for further study.

In the next step, the thermal load profile for each building was computed. The thermal properties were estimated using the available data,

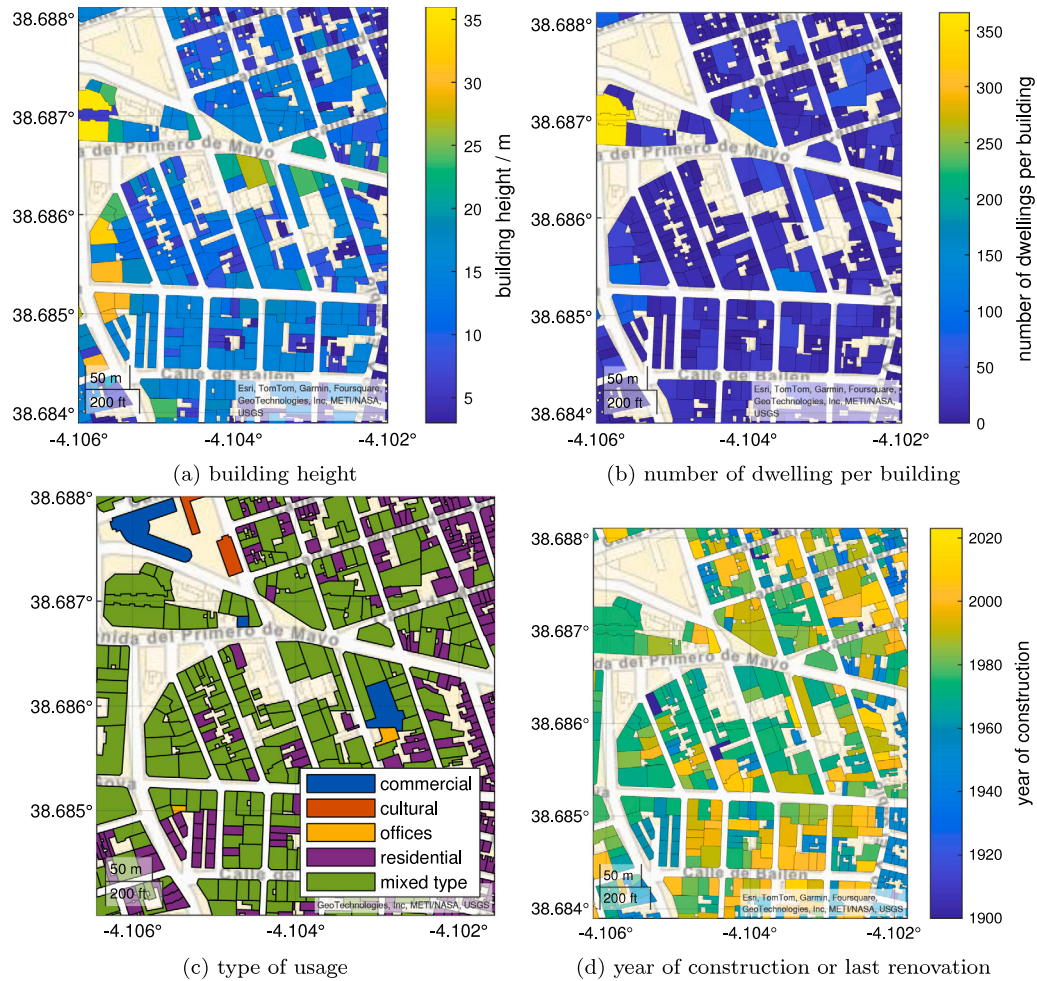


Fig. 9. Different building properties of a small sector of the town, based on OSM and cadaster data.

as outlined in Section 2.2.4. The MCMC method was then employed to generate an active occupancy profile, $A(t)$, with an hourly resolution for both business days and weekends. The transition matrices were derived from Ref. [53]. For the outdoor temperature data, the dataset from Renewables.ninja [62] was utilized. These inputs were subsequently processed through the thermal model, where temperatures and heating demands were iteratively calculated over 8760 steps. This procedure resulted in an hourly heating demand time series for each building. The same process was also applied using data for the nominal heating demand of the buildings, assuming they were retrofitted. The generated dataset can be accessed in Ref. [77]. The total computational time for calculating the time series for the city of 11 725 buildings and 8760 h is approximately 69 s on a standard laptop (Intel i7, 32 GB RAM). A detailed overview of the computational performance can be found in the Supplementary Material [65].

3.3. Results

Fig. 10 presents the calculated total annual heating demand at the building level. The total residential heating demand for the city amounts to 114.2 GW h per year. This value aligns well with the results from the Spanish heat map [40] and the data from the Hotmaps project [39]. By analyzing the building-level data, we can observe that 41 % of the total heating demand is attributed to just 1020 buildings, which represent 10 % of the total number of buildings.

The aggregation of individual heating demand profiles is shown in Fig. 11. Each building has a unique temporal demand profile, reflecting

the diverse daily routines of different societal groups. As more individual profiles are summed up, the resulting curve converges towards a smooth double-peak structure, consistent with patterns observed in the literature [45,60].

The total load profile for all buildings in Puertollano is presented in Fig. 12 for various times throughout the year. The peak heating demand reaches 65.8 MW on a morning in January (the 273rd hour of the year), coinciding with the coldest day of the year.

To illustrate one advantage of using time series data at the building level, we compare two different thermal renovation strategies. First, we randomly select 15 % of the buildings (weighted by residential area; so in total, 15 % of the total residential area is renovated) for thermal retrofitting. For these buildings, improved thermal properties are applied (based on Ref. [30]), and the thermal heating demand time series are recalculated. This process is repeated 50 times with different randomly selected buildings to obtain a statistical distribution. The result is a new yearly demand of (108.3 ± 0.3) GW h (a reduction of 5.2 %) and a peak demand of (62.1 ± 2.0) MW (a reduction of 5.6 %).

We now repeat the analysis deliberately choosing buildings based on their initial thermal performance instead of randomly. By applying energy-saving measures to 15 % of the buildings (weighted by residential area) with the worst thermal performance (according to the revised Energy Efficiency Directive EU/2023/1791 [4]), we achieve a reduction of 13 % in yearly demand and a 15 % reduction in peak demand.

This suggests that smart and selective renovation strategies could be more than twice as effective as uncoordinated actions, which aligns with the findings of Ref. [32]. Fig. 13 compares the time series for the

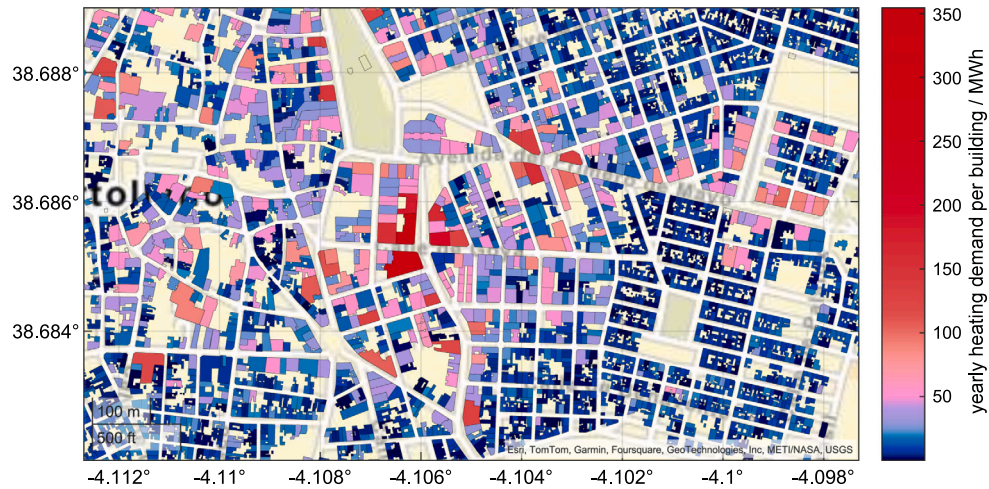


Fig. 10. Calculated total annual heating demand per building with the proposed methodology.

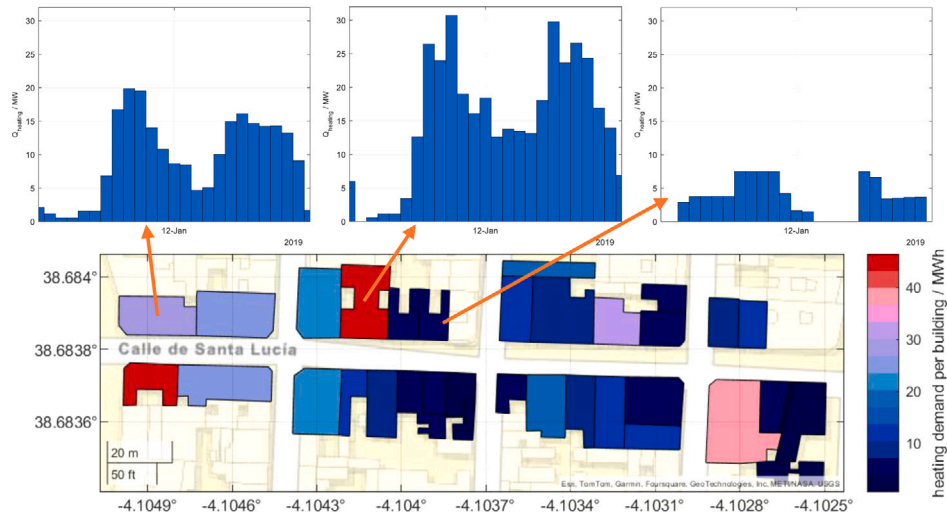


Fig. 11. Illustration of considering diversity among different heating demand profiles and their convergence towards averaged profiles for an increasing number of buildings. The individual profiles depend on the thermal properties of the building and the assigned active occupancy profile.

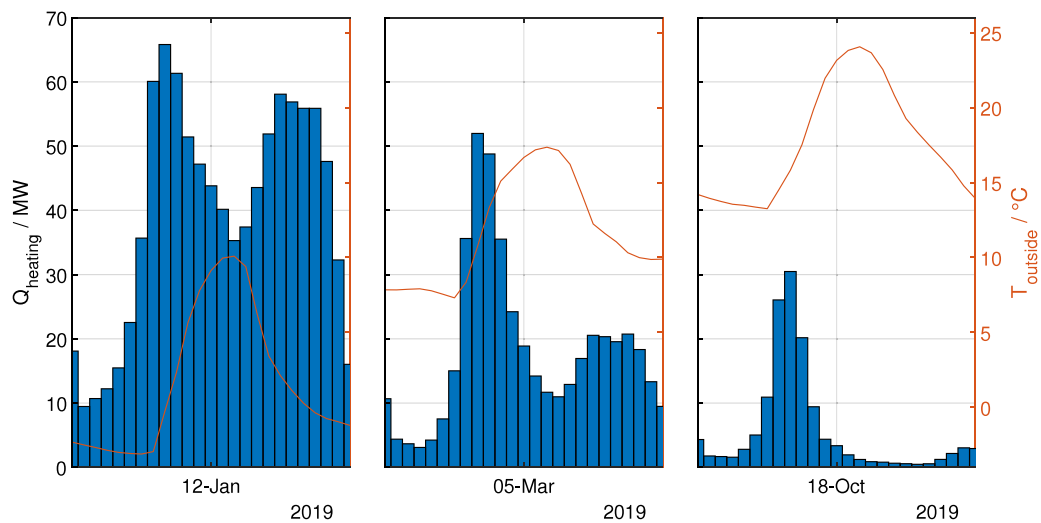


Fig. 12. Aggregated heating demand time series for three different days (0–24 h) and corresponding outdoor temperature.

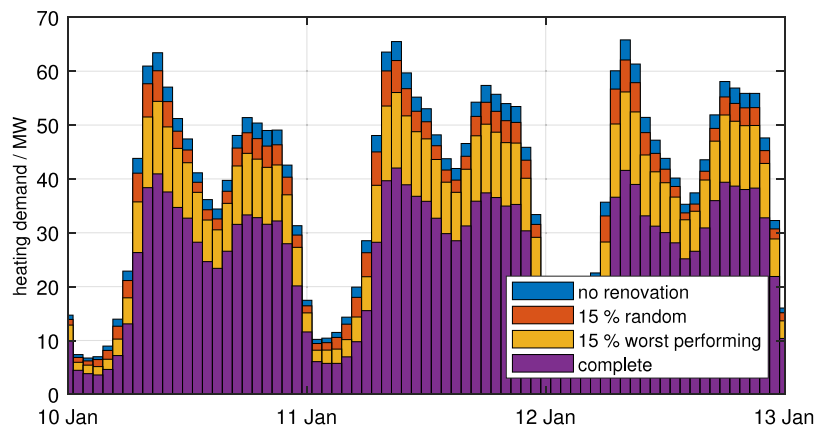


Fig. 13. Comparison of influence of different renovation strategies on the thermal demand time series.

different renovation strategies. It can be seen that the smart approach also contributes to flattening the peak in thermal demand, potentially allowing for a smaller, more cost-effective district heating network design.

4. Conclusion and outlook

In this study, we presented and validated an integrated methodology that generates heat load profiles at the building level, enabling accurate aggregation of individual building data. A key advantage of this approach is the minimal input data required, which allows for broad applicability across Europe. As a result, this method can be used to create datasets that provide highly resolved yearly heating demands and aggregated load profiles for districts on a granular scale.

Such data is invaluable for a variety of applications in smart energy planning. It can help identify clusters of buildings with poor thermal performance for targeted renovation initiatives, facilitate sector-coupled optimization models to decarbonize the residential sector, match intermittent waste heat potentials with optimal heating demand profiles, support district heating grid operators in more detailed planning for grid expansion or optimization, and assist electrical grid operators in better predicting the impact of ongoing electrification of the heating sector on electricity load profiles in the distribution grid. The method also offers full temporal resolution flexibility, assuming outdoor temperature and occupancy profiles are available at the desired time scale.

In the future, improved data availability, particularly regarding the thermal performance of buildings, will further increase the accuracy of our proposed methodology. For example, many dwellings already have precise thermal performance calculations in energy performance certificates, and such data is sometimes available in public registers (e.g., [78]). Making this information accessible for research projects could significantly enhance data quality, though appropriate measures to preserve data privacy must be implemented. Additionally, incorporating other factors such as solar irradiation, wind chill, or city microclimates could additionally improve the model's accuracy.

CRedit authorship contribution statement

Simon Malacek: Writing – original draft, Visualization, Validation, Methodology, Investigation, Conceptualization. **José Portela:** Validation, Supervision, Project administration. **Yannick Werner:** Writing – review & editing, Supervision. **Sonja Wogrin:** Writing – review & editing, Supervision, Resources.

Declaration of Generative AI and AI-assisted technologies in the writing process

During the preparation of this work, the authors used ChatGPT from OpenAI and Grammarly from Grammarly Inc. to enhance readability and perform grammar and spell-checking. After using these tools, the authors reviewed and edited the content. The authors take full responsibility for the content of this publication.

Declaration of competing interest

The authors declare that they have no known competing financial interests or personal relationships that could have appeared to influence the work reported in this paper.

Acknowledgments

Many thanks to David Cardona Vasquez and Alexander Michael Konrad for their preliminary work in this field and the insightful discussions.

This research was supported by funding from the Spanish Centre for the Development of Industrial Technology (CDTI), with Grant Number MIG-20221006 associated with the ATMOSPHERE Project.

Appendix A. Supplementary data

Supplementary material related to this article can be found online at <https://doi.org/10.1016/j.segy.2025.100181>.

Data availability

The dataset generated for the case study and for the validation study can be accessed in Ref. [77].

References

- [1] Eurostat. Simplified energy balances. 2022, http://dx.doi.org/10.2908/NRG_BAL_S.
- [2] Eurostat. Disaggregated final energy consumption in households - quantities. 2022, http://dx.doi.org/10.2908/NRG_D_HHQ.
- [3] Eurostat. Share of energy from renewable sources. 2022, http://dx.doi.org/10.2908/NRG_IND_REN.
- [4] European Parliament. Directive (EU) 2024/1275 of the European Parliament and of the Council of 24 April 2024 on the energy performance of buildings (recast), URL https://eur-lex.europa.eu/legal-content/EN/TXT/?uri=OJ:L_202401275. [Accessed 21 December 2024].
- [5] Walker L, Hischer I, Schlueter A. Does context matter? Robust building retrofit decision-making for decarbonization across Europe. Build Environ 2022;226:109666. <http://dx.doi.org/10.1016/j.buildenv.2022.109666>.

- [6] Pastore LM, Lo Basso G, de Santoli L. How national decarbonisation scenarios can affect building refurbishment strategies. *Energy* 2023;283:128634. <http://dx.doi.org/10.1016/j.energy.2023.128634>.
- [7] Jones SIEE. The need for decarbonisation. *Build Serv Eng Res Technol* 2021;42(3):253–5. <http://dx.doi.org/10.1177/01436244211004788>.
- [8] Díaz-López C, Navarro-Galera A, Zamorano M, Buendía-Carrillo D. Identifying public policies to promote sustainable building: A proposal for governmental drivers based on stakeholder perceptions. *Sustainability* 2021;13(14):7701. <http://dx.doi.org/10.3390/su13147701>.
- [9] Vaishnav P, Fatimah AM. The environmental consequences of electrifying space heating. *Environ Sci Technol* 2020;54(16):9814–23. <http://dx.doi.org/10.1021/acs.est.0c02705>.
- [10] Ssembatya H, Kern JD, Oikonomou K, Voisin N, Burleyson CD, Akdemir KZ. Dual impacts of space heating electrification and climate change increase uncertainties in peak load behavior and grid capacity requirements in Texas. *Earth's Futur* 2024;12(6):e2024EF004443. <http://dx.doi.org/10.1029/2024EF004443>.
- [11] Rosenow J, Hamels S. Where to meet on heat? A conceptual framework for optimising demand reduction and decarbonised heat supply. *Energy Res Soc Sci* 2023;104:103223. <http://dx.doi.org/10.1016/j.erss.2023.103223>.
- [12] Lombardi F, Rocco M, Locatelli S, Magni C, Colombo E, Belussi L, Danza L. Bottom-up lumped-parameters thermodynamic modelling of the Italian residential building stock: Assessment of high-resolution heat demand profiles. *Tec Ital* 2019;63:349–56. <http://dx.doi.org/10.18280/ti-ijes.632-434>.
- [13] Fritz S, Forster J, Rab N. Buildings' energy demand modelling for sustainable decision support. *WIT Trans Ecol Environ* 2015. <http://dx.doi.org/10.2495/sc150271>.
- [14] Akmal M, Fox B, Morrow JD, Littler T. Impact of heat pump load on distribution networks. *IET Gener Transm Distrib* 2014;8(12):2065–73. <http://dx.doi.org/10.1049/iet-gtd.2014.0056>.
- [15] Schwaeppe H, Böttcher L, Schumann K, Hein L, Hälsig P, Thams S, Baquero Lozano P, Moser A. Analyzing intersectoral benefits of district heating in an integrated generation and transmission expansion planning model. *Energies* 2022;15(7). <http://dx.doi.org/10.3390/en15072314>.
- [16] Lips J, Weniger T, Lotz J, Unz S, Beckmann M, Lens H. Optimal expansion planning of energy hubs: The future of CHP sites in Europe. *IFAC-Pap* 2024;58(13):200–5. <http://dx.doi.org/10.1016/j.ifacol.2024.07.483>, 12th IFAC Symposium on Control of Power and Energy Systems - CPES 2024.
- [17] Büttner C, Amme J, Endres J, Malla A, Schachler B, Cußmann I. Open modeling of electricity and heat demand curves for all residential buildings in Germany. *Energy Inform* 2022;5:1–21. <http://dx.doi.org/10.1186/S42162-022-00201-Y/FIGURES/8>.
- [18] Heidenthaler D, Deng Y, Leeb M, Grobbauer M, Kranzl L, Seiwald L, Mascherbauer P, Reindl P, Bednar T. Automated energy performance certificate based urban building energy modelling approach for predicting heat load profiles of districts. *Energy* 2023;278:128024. <http://dx.doi.org/10.1016/j.energy.2023.128024>.
- [19] Malla A. Generation of high spatial and temporal resolution heat demand profiles for Germany [Master's thesis]. *Europa-Universität Flensburg*; 2021.
- [20] Frayssinet L, Merlier L, Kuznik F, Hubert JL, Milliez M, Roux JJ. Modeling the heating and cooling energy demand of urban buildings at city scale. *Renew Sustain Energy Rev* 2018;81:2318–27. <http://dx.doi.org/10.1016/J.RSER.2017.06.040>.
- [21] Swan LG, Ugursal VI. Modeling of end-use energy consumption in the residential sector: A review of modeling techniques. *Renew Sustain Energy Rev* 2009;13:1819–35. <http://dx.doi.org/10.1016/J.RSER.2008.09.033>.
- [22] Gils HC, Cofala J, Wagner F, Schöpp W. GIS-based assessment of the district heating potential in the USA. *Energy* 2013;58:318–29. <http://dx.doi.org/10.1016/J.ENERGY.2013.06.028>.
- [23] OpenStreetMap contributors. OpenStreetMap, URL <https://www.openstreetmap.org/>. [Accessed 21 December 2024].
- [24] Schwanebeck M, Krüger M, Duttman R. Improving GIS-based heat demand modelling and mapping for residential buildings with census data sets at regional and sub-regional scales. *Energies* 2021;14:1029. <http://dx.doi.org/10.3390/EN14041029>.
- [25] Lumbrales M, Diarce G, Martín-Escudero K, Campos-Celador A, Larrinaga P. Design of district heating networks in built environments using GIS: A case study in Vitoria-Gasteiz, Spain. *J Clean Prod* 2022;349:131491. <http://dx.doi.org/10.1016/J.JCLEPRO.2022.131491>.
- [26] Nielsen S, Möller B. GIS based analysis of future district heating potential in Denmark. *Energy* 2013;57:458–68. <http://dx.doi.org/10.1016/J.ENERGY.2013.05.041>.
- [27] Fallahnejad M, Hartner M, Kranzl L, Fritz S. Impact of distribution and transmission investment costs of district heating systems on district heating potential. *Energy Procedia* 2018;149:141–50. <http://dx.doi.org/10.1016/J.EGYPRO.2018.08.178>.
- [28] Meha D, Dragusha B, Thakur J, Novosel T, Duić N. A novel spatial based approach for estimation of space heating demand saving potential and CO₂ emissions reduction in urban areas. *Energy* 2021;225:120251. <http://dx.doi.org/10.1016/J.ENERGY.2021.120251>.
- [29] Martín-Consuegra F, de Frutos F, Oteiza I, Agustín HA. Use of cadastral data to assess urban scale building energy loss. Application to a deprived quarter in Madrid. *Energy Build* 2018;171:50–63. <http://dx.doi.org/10.1016/J.ENBUILD.2018.04.007>.
- [30] Loga T, Stein B, Diefenbach N. TABULA building typologies in 20 European countries — making energy-related features of residential building stocks comparable. *Energy Build* 2016;132:4–12. <http://dx.doi.org/10.1016/J.ENBUILD.2016.06.094>.
- [31] Dall'o' G, Galante A, Torri M. A methodology for the energy performance classification of residential building stock on an urban scale. *Energy Build* 2012;48:211–9. <http://dx.doi.org/10.1016/J.ENBUILD.2012.01.034>.
- [32] Prades-Gil C, Viana-Fons JD, Masip X, Cazorla-Marín A, Gómez-Navarro T. An agile heating and cooling energy demand model for residential buildings. Case study in a Mediterranean city residential sector. *Renew Sustain Energy Rev* 2023;175:113166. <http://dx.doi.org/10.1016/J.RSER.2023.113166>.
- [33] Staffell I, Pfenniger S, Johnson N. A global model of hourly space heating and cooling demand at multiple spatial scales. *Nat Energy* 2023;8(12):1328–44. <http://dx.doi.org/10.1038/s41560-023-01341-5>.
- [34] Meha D, Novosel T, Duić N. Bottom-up and top-down heat demand mapping methods for small municipalities, case Glogoc. *Energy* 2020;199:117429. <http://dx.doi.org/10.1016/J.ENERGY.2020.117429>.
- [35] Calderón C, James P, Urquiza J, McLoughlin A. A GIS domestic building framework to estimate energy end-use demand in UK sub-city areas. *Energy Build* 2015;96:236–50. <http://dx.doi.org/10.1016/J.ENBUILD.2015.03.029>.
- [36] Pampuri L, Cereghetti N, Bianchi PG, Caputo P. Evaluation of the space heating need in residential buildings at territorial scale: The case of Canton Ticino (CH). *Energy Build* 2017;148:218–27. <http://dx.doi.org/10.1016/J.ENBUILD.2017.04.061>.
- [37] Möller B, Wiechers E, Persson U, Nielsen S, Moreno DC. Online web map application and first set of map layers. *Tech. rep.*, 2021, <http://dx.doi.org/10.5281/ZENODO.4785335>.
- [38] Persson U, Möller B, Werner S. Heat roadmap Europe: Identifying strategic heat synergy regions. *Energy Policy* 2014;74:663–81. <http://dx.doi.org/10.1016/j.enpol.2014.07.015>.
- [39] Hotmaps Project Partners. Hotmaps Toolbox, URL <https://www.hotmaps.eu/map>. [Accessed 21 December 2024].
- [40] Instituto para la Diversificación y Ahorro de la Energía (IDAE). Mapa de calor, URL <https://mapadecalor.idae.es/>. [Accessed 21 December 2024].
- [41] Terés-Zubiaga J, González-Pino I, Álvarez-González I, Campos-Celador Á. Multi-dimensional procedure for mapping and monitoring urban energy vulnerability at regional level using public data: Proposal and implementation into a case study in Spain. *Sustain Cities Soc* 2023;89:104301. <http://dx.doi.org/10.1016/J.SCS.2022.104301>.
- [42] Jebaraj S, Iniyas S. A review of energy models. *Renew Sustain Energy Rev* 2006;10:281–311. <http://dx.doi.org/10.1016/J.RSER.2004.09.004>.
- [43] Allegrini J, Orehounig K, Mavromatidis G, Ruesch F, Dorer V, Evins R. A review of modelling approaches and tools for the simulation of district-scale energy systems. *Renew Sustain Energy Rev* 2015;52:1391–404. <http://dx.doi.org/10.1016/J.RSER.2015.07.123>.
- [44] Peacock M, Fragaki A, Matuszewski BJ. Review of heat demand time series generation for energy system modelling. In: Mporas I, Kourtessis P, Al-Habaibeh A, Asthana A, Vukovic V, Senior J, editors. *Energy and sustainable futures*. Cham: Springer International Publishing; 2021, p. 53–60. http://dx.doi.org/10.1007/978-3-030-63916-7_7.
- [45] Koene FG, Eslami-Mossallam BB. Space heating demand profiles of districts considering temporal dispersion of thermostat settings in individual buildings. *Build Environ* 2023;228:109839. <http://dx.doi.org/10.1016/J.BUILDENV.2022.109839>.
- [46] Dang LM, Lee S, Li Y, Oh C, Nguyen TN, Song HK, Moon H. Daily and seasonal heat usage patterns analysis in heat networks. *Sci Rep* 2022;12:1–12. <http://dx.doi.org/10.1038/s41598-022-13030-6>, 2022 12: 1.
- [47] Dang LM, Shin J, Li Y, Tightiz L, Nguyen TN, Song HK, Moon H. Toward explainable heat load patterns prediction for district heating. *Sci Rep* 2023;13:1–13. <http://dx.doi.org/10.1038/s41598-023-34146-3>, 2023 13: 1.
- [48] Maljkovic D, Basic BD. Determination of influential parameters for heat consumption in district heating systems using machine learning. *Energy* 2020;201:117585. <http://dx.doi.org/10.1016/J.ENERGY.2020.117585>.
- [49] Fumo N, Biswas MAR. Regression analysis for prediction of residential energy consumption. *Renew Sustain Energy Rev* 2015;47:332–43. <http://dx.doi.org/10.1016/J.RSER.2015.03.035>.
- [50] Crawley DB, Lawrie LK, Winkelmann FC, Buhl WF, Huang YJ, Pedersen CO, Strand RK, Liesen RJ, Fisher DE, Witte MJ, Glazer J. *EnergyPlus: Creating a new-generation building energy simulation program*. *Energy Build* 2001;33:319–31. [http://dx.doi.org/10.1016/S0378-7788\(00\)00114-6](http://dx.doi.org/10.1016/S0378-7788(00)00114-6).
- [51] Palacios-García EJ, Moreno-Munoz A, Santiago I, Flores-Arias JM, Bellido-Outeirino FJ, Moreno-García IM. A stochastic modelling and simulation approach to heating and cooling electricity consumption in the residential sector. *Energy* 2018;144:1080–91. <http://dx.doi.org/10.1016/J.ENERGY.2017.12.082>.

- [52] Fischer D, Wolf T, Scherer J, Wille-Haussmann B. A stochastic bottom-up model for space heating and domestic hot water load profiles for German households. *Energy Build* 2016;124:120–8. <http://dx.doi.org/10.1016/J.ENBUILD.2016.04.069>.
- [53] Richardson I, Thomson M, Infield D. A high-resolution domestic building occupancy model for energy demand simulations. *Energy Build* 2008;40:1560–6. <http://dx.doi.org/10.1016/J.ENBUILD.2008.02.006>.
- [54] Eurostat. Harmonised European time use surveys, URL <https://ec.europa.eu/eurostat/web/microdata/harmonised-european-time-use-surveys>. [Accessed 21 December 2024].
- [55] Ding X, Ma R, Sun T, Shan M, Wang X, Yang X. Method to elucidate the spatial-temporal characteristics of the intermittent heating demand of rural houses in northern China. *Energy Build* 2023;288:113008. <http://dx.doi.org/10.1016/J.ENBUILD.2023.113008>.
- [56] Fu J, Hu S, He X, Managi S, Yan D. Identifying residential building occupancy profiles with demographic characteristics: Using a national time use survey data. *Energy Build* 2022;277:112560. <http://dx.doi.org/10.1016/J.ENBUILD.2022.112560>.
- [57] Ruhnau O, Hirth L, Praktijnjo A. Time series of heat demand and heat pump efficiency for energy system modeling. *Sci Data* 2019;6(1):189. <http://dx.doi.org/10.1038/s41597-019-0199-y>.
- [58] Ruhnau O, Muesel J. When2Heat heating profiles. 2023, <http://dx.doi.org/10.25832/WHEN2HEAT/2023-07-27>, Type: dataset.
- [59] Berger M, Worlitschek J. A novel approach for estimating residential space heating demand. *Energy* 2018;159:294–301. <http://dx.doi.org/10.1016/J.ENERGY.2018.06.138>.
- [60] Clegg S, Mancarella P. Integrated electricity-heat-gas modelling and assessment, with applications to the great britain system. Part I: High-resolution spatial and temporal heat demand modelling. *Energy* 2019;184:180–90. <http://dx.doi.org/10.1016/J.ENERGY.2018.02.079>.
- [61] Glossary: Nomenclature of territorial units for statistics (NUTS), URL [https://ec.europa.eu/eurostat/statistics-explained/index.php?title=Glossary:Nomenclature_of_territorial_units_for_statistics_\(NUTS\)](https://ec.europa.eu/eurostat/statistics-explained/index.php?title=Glossary:Nomenclature_of_territorial_units_for_statistics_(NUTS)).
- [62] Staffell I, Pfenninger S. Renewables.ninja. URL <https://www.renewables.ninja/>. [Accessed 21 December 2024].
- [63] European Parliament. Richtlinie - 2007/2 - EN - EUR-Lex / INSPIRE, URL <https://eur-lex.europa.eu/legal-content/DE/ALL/?uri=celex%3A32007L0002>. [Accessed 21 December 2024].
- [64] Raifer M. overpass turbo, URL <https://overpass-turbo.eu/>. [Accessed 21 December 2024].
- [65] Malacek S, Portela J, Werner Y, Wogrin S. Supplementary material to generating building- level heat demand time series by combining occupancy simulations and thermal modeling. 2025, <http://dx.doi.org/10.3217/0b20r-jrx54>.
- [66] Goeke J. Gebäude als thermischer Energiespeicher. *Thermische Energiespeicher der Gebäudetechnik* 2021;493–550. http://dx.doi.org/10.1007/978-3-658-34510-5_16.
- [67] DIN. Vereinfachte Heizlastberechnung nach DIN 4701. URL <https://www.ibo-plan.de/heizlastberechnung/andere-berechnungsverfahren/heizlastberechnung-nach-hea-kurzverfahren/vereinfachte-heizlastberechnung-manuell.html>. [Accessed 21 December 2024].
- [68] Firlag S, Zawada B. Impacts of airflows, internal heat and moisture gains on accuracy of modeling energy consumption and indoor parameters in passive building. *Energy Build* 2013;64:372–83. <http://dx.doi.org/10.1016/j.enbuild.2013.04.024>.
- [69] Unternährer J, Moret S, Joost S, Maréchal F. Spatial clustering for district heating integration in urban energy systems: Application to geothermal energy. *Appl Energy* 2017;190:749–63. <http://dx.doi.org/10.1016/J.APENERGY.2016.12.136>.
- [70] Dochev I, Seller H, Peters I. Assigning energetic archetypes to a digital cadastre and estimating building heat demand. An example from hamburg, Germany. *Environ Clim Technol* 2020;24:233–53. <http://dx.doi.org/10.2478/RTUECT-2020-0014>.
- [71] Li X, Zhou Y, Yu S, Jia G, Li H, Li W. Urban heat island impacts on building energy consumption: A review of approaches and findings. *Energy* 2019;174:407–19. <http://dx.doi.org/10.1016/j.energy.2019.02.183>.
- [72] Yang X, Peng LLH, Jiang Z, Chen Y, Yao L, He Y, Xu T. Impact of urban heat island on energy demand in buildings: Local climate zones in Nanjing. *Appl Energy* 2020;260:114279. <http://dx.doi.org/10.1016/j.apenergy.2019.114279>.
- [73] Iberdrola S. Puertollano green hydrogen plant - Iberdrola, URL <https://www.iberdrola.com/about-us/what-we-do/green-hydrogen/puertollano-green-hydrogen-plant>. [Accessed 21 December 2024].
- [74] elespanolcom. Iberdrola desarrollará en Puertollano una red de calefacción desde su planta de hidrógeno verde, URL https://www.elespanol.com/eldigitalcastillalamancha/economia/empresas/20220412/iberdrola-desarrollara-puertollano-calefaccion-planta-hidrogeno-verde/664433835_0.html. [Accessed 21 December 2024].
- [75] Ministerio de Hacienda / Spain. Sede Electrónica del Catastro - Inicio, URL <https://www.sedecatastro.gob.es/>. [Accessed 21 December 2024].
- [76] Servicios web libres de la Sede Electronica del Catastro - WebservicesLibres, URL <https://www.catastro.hacienda.gob.es/ws/WebservicesLibres.pdf>.
- [77] Malacek S. Building-level heat demand time series derived from open data: Case study dataset. 2024, <http://dx.doi.org/10.3217/64x6f-j9779>.
- [78] Statistik Austria. Energieausweisdatenbank (EADB), URL <https://www.statistik.at/datenbanken/adress-gebaeude-und-wohnungsregister/energieausweisdatenbank-eadb>. [Accessed 21 December 2024].